

Modeling-based Development of an Enantioselective Hydrogenation Reaction of a Sitagliptine Intermediate

I. Šoštarić,^a I. Nežić,^a F. Jović,^{a,*} E. Marčelić,^a E. Meštrović,^a and S. Zrnčević^b

^aPLIVA Croatia LTD, TAPI Croatia, TAPI R&D, API Pilot, Prilaz baruna Filipovića 25, 10000 Zagreb, Croatia

^bFaculty of Chemical Engineering and Technology, Department of Reaction Engineering and Catalysis, Savska cesta 16, Zagreb, Croatia

Original scientific paper

Received: April 11, 2013

Accepted: September 9, 2013

This work presents a quality by design (QbD) driven approach to the plan of experiments and reaction modeling that was effective in obtaining enhanced process knowledge and defining a design space for an active pharmaceutical ingredient (API) manufacturing process. Engineering aspects of the process were explored by process modeling using computer predictive process simulators. QbD approach is presented on a case study of the process development of the sitagliptine synthesis step. The process involves an enantioselective hydrogenation step. Based on the proposed reaction mechanism and by combining the heat and mass transfer, thermodynamics, and the kinetics of the reactions, the API quality specifications (enantiomeric purity, impurity levels) are described across the modeling of process space. This process space was defined through target specifications, practical operating conditions for scale-up, and plant control capabilities. Model predictions were verified with results obtained in the laboratory, and at pilot plant scale.

Key words:

Active pharmaceutical ingredient (API), Quality by Design (QbD), design space, modeling, sitagliptine

Introduction

The use of process models to speed up the development and optimize the design and operation of integrated processes has increased dramatically in recent years in the pharmaceutical industry.^{1,2} All aspects of modeling appliance (and process simulators as well) in process development need some guidelines. That is why different regulatory agencies (such as U.S. Department of Health and Human Services, Food and Drug Administration) have developed a method for evaluating new drug applications, especially the chemistry, manufacturing, and process controls. This approach is described in relevant covering topics given by the International Conference on Harmonisation of Technical Requirements for Registration of Pharmaceuticals for Human Use (ICH). There is an endorsed guide for ICH implementations Q8, Q9 and Q10, describing a new scientific development approach that supplements the existing one.³ It is a concrete and practical implementation of some underlying concepts and principles outlined in quality by design (QbD) initiatives.⁴

The QbD initiative aims to ensure pharmaceutical product quality via scientific process understanding, risk management, critical quality attribute

(CQA) control strategies, and multivariate design space definition.^{3–10} The QbD was described and some of its elements identified.⁹ Process parameters and quality attributes were identified for each unit operation. The use of QbD was contrasted with the evaluation of product quality by testing alone. The QbD is a systemic approach to pharmaceutical development. It means designing and developing manufacturing processes to ensure predefined product quality and process robustness.¹⁰ The use of mechanistic models in process development has multiple benefits. Mechanistic models enable systematic analysis of experimental data and quantification of intrinsic and/or scale-dependent process attributes.

Computer aided process design and simulation tools have been successfully used in the pharmaceutical industry. Many authors have worked on modeling and developing API production process with QbD methodology, which can be referred to development of reaction kinetics of the manufacturing process of: Torcetrapib,¹¹ Ibipinabant,¹² recombinant protein¹³ and different drug substances,¹⁴ for the control of genotoxic impurities in the manufacturing process of a drug substance,¹⁵ as well as to the development of crystallization processes.^{16–18} According to current QbD FDA submission statistics, the number of QbD new molecular entity applications rises significantly.¹⁹

*Corresponding author: franjo.jovic@pliva.com

The primary emphasis of this article is on the role of modeling using process simulators and quality by design method in expediting process development of an enantioselective hydrogenation reaction of a sitagliptine intermediate. Sitagliptin phosphate monohydrate ((R)-4-oxo-4-[3-(trifluoromethyl)-5,6-dihydro [1,2,4]triazolo [4,3-a]pyrazin-7(8H)-yl]-1-(2,4,5-trifluorophenyl)butan-2-amine phosphate monohydrate, *Januvia*TM) is an oral antihyperglycemic (antidiabetic drug) of the dipeptidyl peptidase-4 (DPP-4) inhibitor class.²⁰ This enzyme-inhibiting drug is used either alone or in combination with other oral antihyperglycemic agents (such as metformin or a thiazolidinedione) for treatment of diabetes mellitus type 2.

The asymmetric hydrogenation route is the last generation of sitagliptin synthesis that was published.²¹ As a key step in the proposed synthesis preparing homogeneous catalytic asymmetric reduction of enamine, the main emphasis of this work was placed on that reaction. For catalysts it usually uses Rh, Ru, and Ir complexes which are all known for effecting olefin hydrogenations, in combination with bidentate phosphine ligands from three major categories: C2 symmetric phosphines, non-C2 symmetric phosphines with a ferrocene core, and chiral phospholanes. In this step, enamine was asymmetrically hydrogenated and then crystallized as its free base. Using the complex generated in situ from [Rh(COD)Cl]₂ and *t*-Bu Josiphos as catalyst in methanol as solvent, enamine is hydrogenated at 7 bar H₂ and 50 °C to provide sitagliptin. A conversion of 99 % with selectivity of 95 % *ee* was obtained. These results demonstrated that the *N*-acyl protecting group is not required under Rh catalyzed conditions for this asymmetric transformation. Under the same conditions, iridium catalysts showed some reactivity but no selectivity. All ruthenium based catalysts gave very low reactivity.²¹

According to the criterion of efficiency, Ru(COD)Cl₂/BINAP was used in the development as an available catalyst (precursor + chiral ligand). According to the literature²¹ this catalyst has inferior activity compared to Josiphos based catalysts (<20 % of conversion). After the selection of the catalyst, other reaction parameters were optimized. A solvent screen revealed that the alcohols (e.g. methanol) in combination with organic acid (e.g. acetic acid) were possible solvents to perform reaction. Due to the fact that reactant degradation is observed in acidic conditions, it was observed that 2,2,2-trifluoroethanol (TFE) was a much better solvent. It was also found that the reaction parameters, such as temperature and pressure, significantly influence reaction profile.^{22–28}

The main aim of this paper is to summarize the development of homogeneous catalytic asymmetric

reduction of the sitagliptine intermediate enamine. Along with the criterion of catalyst enantioselectivity, the process should also take into account other factors, such as scale up and feasibility of the process. It is also important to maintain the activity and stability of the catalyst. The ability to regenerate solvents is also important. The influence of process parameters, such as heat and mass transfer, reaction kinetics, catalyst activity, selectivity, and stability are explored. Reaction mechanism has been studied and a kinetic model has been developed for optimization of catalytic reactors. Scientific research emphasis is on examining the influence of catalyst (metal precursor + chiral ligand), temperature and pressure on the yield and selectivity of the reaction by response surface of QbD methodology.

Experimental

To study the influence of various process parameters on the activity, selectivity and stability of the catalyst, an automated batch reactor, $V = 300 \text{ cm}^3$ (*FlexyLab FT-5, Systag*) was used. The reactor is equipped with a stirrer and a system for taking liquid samples without opening the reactor and stopping reactions. It is connected to a thermostat to regulate and maintain the temperature. An automated system for nitrogen or hydrogen pressurization is connected to reactor with measuring the flow rate and the total consumption of hydrogen (*Bronkhorst*). The reactor is part of a *Systag* system for parallel optimization process of 6 independent reactor units controlled via computer, with the ability to manage and control all process parameters (pressure, temperature, stirrer speed, pH, fluid dispensing). All parameter values are monitored, and the system has automatic acquisition of data.

Scale up of hydrogenation reaction on the industrial scale was conducted in batch reactor, $V = 40.0 \text{ dm}^3$ (*Pfandler*). The reactor is made of steel and is glass-lined, equipped with the gas supply system (hydrogen and nitrogen). The reactor is heated by the reactor jacket (steam and water mixture) and equipped with a sampling system.

The process step of the sitagliptine production which includes the catalytic enantioselective hydrogenation reaction of (*Z*)-ethyl 3-amino-4-(2,4,5-trifluorophenyl) but-2-enoate was developed. The commercial catalyst used in the process was supplied by *Johnson Matthey*, UK. It is a complex catalyst consisting of a metal part Ru(COD)Cl and ligand (*R*)-BINAP. The solvent trifluoroethanol (TFE) and intermediate were supplied by *Pliva Ltd.*, Croatia. Compressed hydrogen was supplied by *Messer*, Germany.

In the reactors, a certain amount of reactant, (Z)-ethyl 3-amino-4-(2,4,5-trifluorophenyl) but-2-enoate, solvent (TFE), and catalysts (metal + chiral ligand) were added. The reactors were sealed, and the appropriate rotating speed of stirrer to the reaction mixture was applied. The reactors were inertized three times with nitrogen flow to remove oxygen from the reactors, and then washed with hydrogen. The reaction mixture was then heated up to working temperature. When the operating temperature was reached, the reactor was pressurized up to working value and that moment was taken as the beginning of the reaction (at which $t = 0$). Hydrogen pressure in the reactor was maintained constant throughout the reaction. Reaction was explored by varying the process parameters to obtain the appropriate purity (chemical and optical) of the product and develop a robust process that can be applied on an industrial scale.

Preliminary design of experiments

During preliminary screening experiments (screening of various catalyst, solvents and promoters), the reaction system (Ru/Binap in TFE) was chosen for further development. Separation of enantiomers is difficult since they have the same physical properties; emphasis during development of the hydrogenation reaction was put on satisfactory enantiomeric purity. Isolation was further optimized to achieve chromatographic purity of the product. All impurities are the result of hydrolysis of enamine to the β -ketoester, and consequently were reduced to corresponding alcohols. Impurities do not have amino group and cannot form salts; therefore, isolation of product through oxalic salt was chosen. The target function was defined by product specifications, target product profile which was HPLC optical purity (NLT 98 %), and chemical purity, (NLT 93 %).

Two types of analyses were conducted on HPLC *Agilent Technologies* (models 1100 and 1200) with DAD detector. Enantiomeric purity was analyzed on *Daicel, Chiralcel AD-H* column with diluents (Hexane:Ethanol = 70:30) + 0.1 % DEA. Analytical run-time was 40 minutes, injection volume 10 μL , flow rate 1 mL min^{-1} , detector 210 nm, and column temperature 20 $^{\circ}\text{C}$. Chromatographic purity, product concentration, and impurity profile were measured according to the developed methods on Waters Phenyl, 3.5 μm , 4.6 x 150 mm column, using buffer (20 mM ammonium dihydrogen phosphate, and 2 mmol L^{-1} sodium pentasulfonate monohydrate adjusted to pH 6.0 with ammonium hydroxide) and ACN in ratio = 87:13 with time gradient method, injection volume 10 μL , flow rate 0.8 mL min^{-1} , detector 268 nm (BW 4 nm; ref. 360 nm, BW 100 nm), and column temperature 35 $^{\circ}\text{C}$.

Based on target product profile, the critical quality attributes (CQAs) were determined. For the reaction of reduction of enamine CQA is enantiomeric purity. Among all process parameters, statistical analysis (*Correlation* – statistical Toolbox in *Excel*) gives measurement of the impact of critical process parameters (CPPS) on CQAs. The performed risk assessment analysis led to the conclusions that 3 factors could be significant for the enantiomeric purity response. Table 1 summarizes explored parameters, and their significance was ranked according to their significance to the CQA, and their interactions assessed. Statistical analysis is used to extract critical process parameters (CPPs), namely, temperature of reaction mixture as the most critical. Modeling base prediction with parameter estimation was performed with software *DynoChem*[®] (Scale-up Systems, Ltd., Ireland).

Table 1 – Correlation matrix of process parameters in a catalytic asymmetric reduction of (Z)-ethyl 3-amino-4-(2,4,5-trifluorophenyl) but-2-enoate

	Reaction temperature / $^{\circ}\text{C}$	Hydrogen pressure / bar	Catalyst quantity / mol %	HPLC / opt. purity %
Reaction temperature / $^{\circ}\text{C}$	1.000			
Hydrogen pressure / bar	0.063	1.000		
Catalyst quantity / mol %	0.070	-0.117	1.000	
HPLC / opt. purity %	0.959	0.047	0.044	1.000

Design of experiments

DoE methodology is used in the QbD paradigm to define Design Space and Critical Process Parameters (CPPs), and assess process robustness. Experimental design (full factorial design + replicated experiments and center points) was conducted to understand impact of chosen factors which could influence enantiomeric and chromatographic purity (response variables) at 3 levels. Additionally, mass transfer coefficient, $k_L a$ for Scale Up purposes was added in case of mass transfer limited process. For calculations of gas dispersion and mass transfer in gas-liquid mixing systems, the software *VisiMix* (VisiMix, Ltd., Israel) was used. Mathematical modeling is based on a set of original physical models.^{29–31} It is assumed that concentration of the hydrogen component of the gas or its solubility is low, and the outlet value for the volume flow rate of gas is equal to its inlet value. Mixing tanks, under these assumptions, are used for gas-liquid mass transfer operations mainly when the mass transfer rate is

limited due to the high film resistance in the liquid phase. Therefore, only the liquid phase mass transfer was taken into account, and the overall mass transfer coefficient was assumed to be equal to the liquid side film coefficient.

Kinetic data was obtained by changing various parameters that influence the reaction rate (CPPs). Samples of the reaction mixture (0.2 cm³) were taken at certain time intervals until the end of reaction criteria was achieved (NMT 1 % starting material). Samples were prepared (quenched) with diluents to a volume 25 cm³. Chromatographic purity was explored in defined process space (Table 2.)

Table 2 – Critical process parameters (CPPs) included in the process analysis

Parameter	Experimental design levels
Temperature	Low, 60 °C
	Center, 70 °C
	High, 80 °C
Hydrogen pressure	Low, 2 bar
	Center, 6 bar
	High, 15 bar
Catalyst mass, mol Eqv. to Comp 1	Low, 0.75 mol %
	Center, 1.00 mol %
	High, 1.25 mol %
Mass transfer coefficient, $k_L a$	Low, 0.001 s ⁻¹
	Center, 0.010 s ⁻¹
	High, 0.100 s ⁻¹

Parameter estimation and evaluation of the model

F-Statistics of model agreement is used for experimental data fitting. The *F*-statistic is the ratio of the variation explained by the model to the variation unexplained by the model. The sum of squares (SSQ) is a measure of the closeness of the model results to the data. A high relative SSQ value indicates that the profile is poorly fitted. The Durbin-Watson statistic was used to obtain the first order autocorrelation of residuals, and for 95 % confidence levels, $-0.25 < D < 0.25$ indicates little autocorrelation. Skewness is a measure of the symmetry of the distribution of residuals. A good model fit should have a skewness close to zero (a normal distribution has zero skewness) indicating that the residuals are normally distributed.

Experimental data were analyzed by simultaneous numerical methods for solving partial differen-

tial equations with Rosenbrock method (with accuracy of 0.001) and simultaneous evaluation of model parameters by Levenberg-Marquardt algorithm (with fitting tolerance of 0.0001) in the *Dynochem* software package.

On the basis of the existing process knowledge, the first three of four factors (Table 2) were selected for model building and translated into the above-mentioned kinetic model. A model built from these factors adequately describes the stereoselective hydrogenation reaction across the existing data set (Figs. 4, 5, Table 5). An additional factor which describes the mass transfer (mixing) is incorporated into the model. Mechanistically, hydrogen diffuses from headspace to bulk liquid phase in order to react with reactant. The reaction is performed on the solvent reflux on which hydrogen solubility is low, so mass transfer could be a determining step. Catalytic reactions involve adsorption/desorption steps which could also be rate determining steps.

Results and discussion

Reaction mechanism

Product (*R*)-ethyl 3-amino-4-(2,4,5-trifluorophenyl) butanoate (**Compound 2** – *RT* = 10.022 min, *RRT* = 1.0, Fig. 2) was prepared by homogeneous stereoselective hydrogenation of (*Z*)-ethyl 3-amino-4-(2,4,5-trifluorophenyl)but-2-enoate (**Compound 1**, *RRT* = 2.48, Fig. 2) in 2,2,2-trifluoroethanol (TFE) with Ru(COD)Cl/(*R*)-BINAP (**Ru/BINAP**) as a catalyst (Fig. 1). It was observed that **Compound 1** was not stable in the acidic conditions and converted into previous step intermediate, which was ethyl 4-(2,4,5-trifluorophenyl)-3-oxobutanoate (**Impurity 1**, *RRT* = 2.48, Fig. 2). **Impurity 1** was subsequently hydrogenated into different process impurities which could be seen on representative chromatogram (*RRT* = 2.67 – 3.65, Fig. 2). The pseudo-impurity was used for kinetic analysis as a sum of all other impurities produced in the reaction according to the reaction mechanism (**Impurity 2**). (*R*)-trifluoroethyl 3-amino-4-(2,4,5-trifluorophenyl) butanoate (**Compound 3**, *RRT* = 1.50, Fig. 2) is a process related byproduct formed during the reaction of hydrogenation by reaction transesterification – the formation of trifluoroethanol ester from the product **Compound 2**. Mix of **Compound 2** and **3** was isolated and purified as oxalate salt product (**Compound 4**). This product was converted in the next step by reaction ester hydrolysis into 3-[[*(tert*-butoxy) carbonyl] amino}-4-(2,4,5-trifluorophenyl) butanoic acid (**Compound 5**). The optical purity of the product is referred to as (*R*)-stereoisomer of **Compound 2**

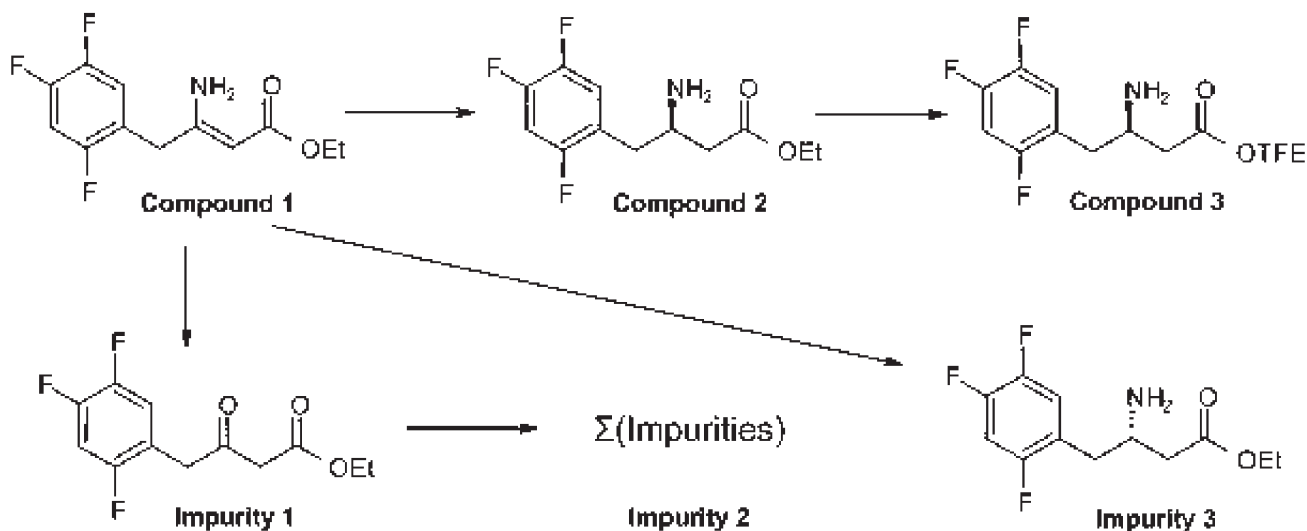


Fig. 1 – Reaction mechanism

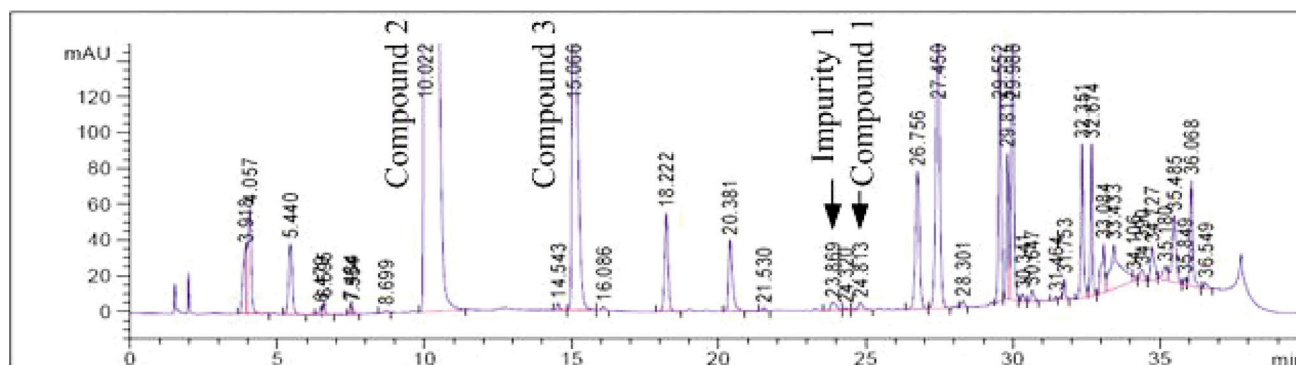


Fig. 2 – Representative chromatogram of hydrogenation reaction mixture

in the reaction mixture. (*S*)-stereoisomer of **Compound 2** will be referred to as **Impurity 3**. All yields are referred to isolated product (**Compound 5**).

Reaction kinetics

Based on the proposed reaction mechanism and reaction path, the kinetic model of complex hydrogenation reaction is derived. It consists of individual kinetic reaction steps (Fig. 3). To analyze and improve the process, the reaction mechanism and kinetics was developed using *DynoChem* software.

Calculated mass transfer coefficient for H₂/TFE system at 60 – 80 °C was estimated at $k_L a = 0.00961 \text{ s}^{-1}$. Total mass transfer rate is given by equation (1):

$$dc(\text{H}_2)/dt = k_L a (c^*(\text{H}_2) - c(\text{H}_2)) \quad (1)$$

A temperature dependent solubility of hydrogen based on Henry's law (Eq. (2) and (3)) was estimated according to DIPPR solvent database found in the *DynoChem* hydrogen solubility utility:

Headspace	H ₂ , TFE
Bulk liquid	$k_L a$ Henry
<i>Catalyst complex formation</i>	Ru + BINAP > Ru-BINAP
<i>Catalyst activation</i>	Ru-BINAP + H ₂ > Ru-BINAP*
<i>Substrate degradation</i>	Comp 1 > Imp 1
<i>Impurity formation</i>	Imp 1 + H ₂ > Imp 2
<i>Substrate adsorption</i>	Ru-BINAP* + Comp 1 > Ru-BINAP-Comp 1
<i>API product formation</i>	Ru-BINAP-Comp1 + H ₂ > Ru-BINAP-Comp 2
<i>Impurity formation</i>	Ru-BINAP-Comp1 + H ₂ > Ru-BINAP-Imp 3
<i>Product desorption</i>	Ru-BINAP-Comp2 > Ru-BINAP*+Comp 2
<i>Impurity desorption</i>	Ru-BINAP-Imp3 > Ru-BINAP* + Imp 3
<i>Transesterification</i>	Comp 2 + TFE > Comp 3
	Solvent TFE

Fig. 3 – Process chemistry overview. Suggested mechanism of homogeneous stereoselective hydrogenation of (*Z*)-ethyl 3-amino-4-(2,4,5-trifluorophenyl)but-2-enoate (**Comp. 1**)

$$c^*(\text{H}_2)/\text{kg m}^{-3} = K_{\text{Henry}} p(\text{H}_2)/\text{bar} \quad (2)$$

$$K_{\text{Henry}} = H_{\text{ref}} \cdot \exp(-A_1 \cdot (1/T - 1/T_{\text{ref}})) \quad (3)$$

Reaction kinetics is also affected by temperature which is described with Arrhenius equation:

$$k = k_{\text{ref}} \exp(-E_A / R \cdot (1/T - 1/T_{\text{ref}})) \quad (4)$$

where the values of $k = k_{\text{ref}}$ at a default reference temperature, $T_{\text{ref}} = 20^\circ\text{C}$.

For reaction kinetics, two reaction orders can be assumed, in a reaction $A \rightarrow P$, the order of reaction on a species A can be first or second, and the equation for reaction rate is:

$$r_A = k c_A; \quad \text{or} \quad r_A = k c_A^2 \quad (5)$$

where the rate constant units are s^{-1} or $\text{L mol}^{-1} \text{s}^{-1}$.

The goal for experimentation was to develop quantitative understanding of drug substance critical quality attributes (CQAs) in terms of input material attributes and API processing parameters. Several API substance CQAs were identified: optical purity, impurity profile, and total efficiency was optimized as well.

The experimental plan supported the development of a mechanistic model for **Compound 2** formation and degradation of the intermediate **Compound 1** to **Impurity 1**, and its further hydrogenation to the impurities of **Impurity 2**. Table 2 presents factors which are critical for process development (CPPs). The responses were in-process amounts of residual input materials, product and impurities (Fig. 2). Levels for factors were selected to provide sufficient magnitude of variation in the responses across different conditions (Table 2), so that model parameters could be estimated accurately. Amount of solvent was maintained as low as possible to dissolve **Compound 1** (5 volumes of TFE/ relative to **Comp. 1** – V/w), and reach homogeneous reaction conditions.

The development of hydrogenation step of **Compound 1** to **Compound 2** at different temperatures (60–80 °C) was tested at 6 bar of hydrogen pressure. From the results (Table 3) it may be concluded that the reaction at lower temperatures de-

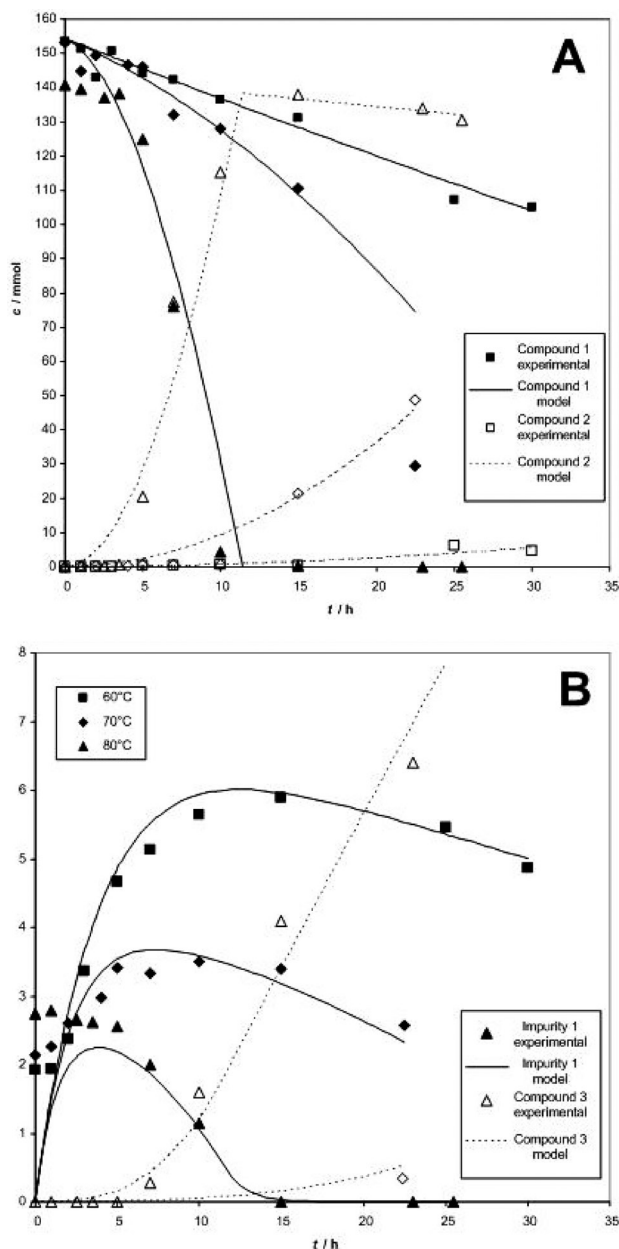


Fig. 4 – Influence of temperature on reaction profile: A) Conversion of **Compound 1** (full line) to **Compound 2** (dashed line); B) Impurity formation of **Impurity 1** (full line) and byproduct formation **Compound 3** (dashed line) at 60° (■), 70° (◆), and 80 °C (▲) (reaction conditions: $p(\text{H}_2) = 6$ bar; $w(\text{catalyst}) = 1$ mol %, $V(\text{reaction mixture}) = 200$ cm³)

Table 3 – Optical purity of isolated product, **Compound 4** – oxalate salt of **Compound 2** and **3** as a function of reaction temperature

Reaction temperature / °C	HPLC / chrom. purity %		HPLC / opt. purity %
	Compound 2	Compound 3	
60	63.2	1.9	83.8
70	65.1	9.4	98.3
80	89.7	8.9	98.4

creases the optical purity of the product (weight percentage of (*R*)-stereoisomer – **Compound 2** in mixture with (*S*)-stereoisomer – **Impurity 3**) in the reaction mixture, and also decreases the reaction rate (Fig. 4A). According to the literature, the reaction temperature was found to be an important factor.²⁰ At 80 °C in TFE with 1 mol % of catalyst loading, the reaction takes about 15 h to complete (Fig. 4). The reaction proceeded very slowly at lower temperatures (at temperature of 60 °C reaction takes more than 30 hours – Fig. 4A). To make a clean regression of all proposed parameters in reac-

tion mechanism (Fig. 3) for complex hydrogenation reaction, kinetic experiments need to be performed. The samples were collected at different time intervals to generate concentration vs. time data (Fig. 4, 5). Conversion of **Compound 1** to product significantly increases with temperature (Fig 4A). Thermal degradation of **Compound 1** to **Impurity 1** slowly rises with temperature (at $t = 0$, Fig. 4B). **Impurity 1** quantity in reaction conditions (at $p(\text{H}_2) = 6$ bar) decreases with temperature due to the faster hydrogenation reaction (formation of **Impurity 2**). These process-related impurities mostly remain in the mother liquor and do not affect product purity but decrease reaction yield. Formation of **Compound 3** is strongly dependent on temperature.

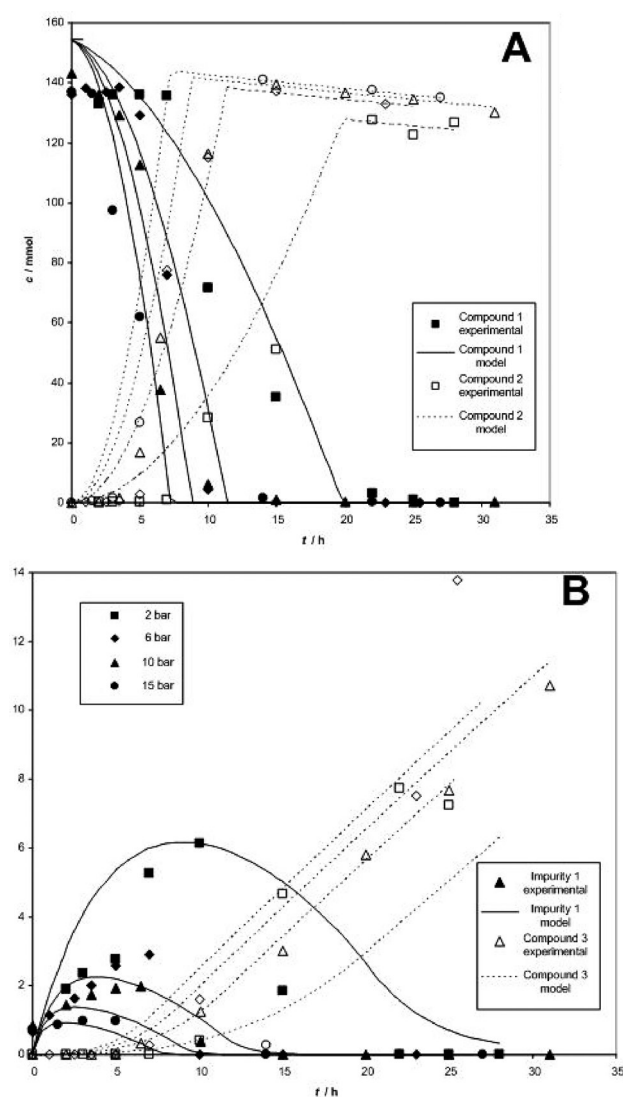


Fig. 5 – Influence of hydrogen pressure on reaction profile: A) Conversion of **Compound 1** (full line) to **Compound 2** (dashed line) B) Impurity formation of **Impurity 1** (full line) and byproduct formation **Compound 3** (dashed line) at 2 (■), 6 (◆), 10 (▲), and 15 (●) bar (reaction conditions: $T = 80$ °C; $w(\text{catalyst}) = 1$ mol %, $V(\text{reaction mixture}) = 200$ cm³)

The reaction of hydrogenation was tested at 80 °C and at different pressures of hydrogen (2.0–15.0 bar). It is concluded that at higher pressures (> 6 bar) there is no high influence on the reaction kinetics (Fig. 4A); therefore, there is no need for higher pressure. At lower pressure, it is observed that optical purity is the same, but reaction lasts longer. According to the literature, the reaction rate increased proportionally with pressure while the enantioselectivity was not pressure dependent³². Increasing the pressure from 2 to 15 bar increased the reaction rate, and decreased the induction time (Fig. 5A). Hydrogenation of **Impurity 1** increases with hydrogen pressure (Fig. 5B). Hydrogen pressure does not affect formation of **Compound 3**, the rate is not dependent on hydrogen pressure.

Quantity of catalyst was tested in standard reaction conditions (80 °C, 6 bar). The results are presented in Table 4. With less quantity of catalyst, slightly lower optical purity was observed in comparison to the standard reaction conditions.

Table 4 – Optical purity of isolated product, **Compound 4** – oxalate salt of **Compound 2** and **3** as a function of catalyst quantity

Catalyst quantity	HPLC / chrom. purity %		HPLC / opt. purity %
	Comp 2	Comp 3	
Ru/BINAP 1:1.2; 1 mol % Ru to Comp 1	80.8	6.6	98.2
Ru/BINAP 1:1; 0.75 mol % Ru to Comp 1	89.5	9.3	98.2
Ru/BINAP 1:1; 1.25 mol % Ru to Comp 1	82.3	7.0	97.8
Ru/BINAP 1:1; 1 mol % Ru to Comp 1	89.5	8.5	98.5

According to Clausen *et al.*²⁷ product desorption is a slow step in asymmetric hydrogenation of a β -enamine amides. Our results showed that in stereoselective hydrogenation of sitagliptine, product desorption is also a rate determining step (r.d.s.), with $k_7 = 0.0139$ s⁻¹ (Table 5.).

Prolonged induction time is described with two constants – catalyst complex formation and activation, but there are no analytical data to support these two reactions. According to the literature³³ the reduction of β -ketoesters with Ru(II)-BINAP obtained with enantioselectivity is nearly always greater than 97 % and typically accomplished in 2–8 h, which is similar to our results. Substrate degradation of **Compound 1** to **Impurity 1** is thermal degradation ($E_{A,3} = 77.96$ kJ mol⁻¹) and degradation rate is slow with constant $k_3 = 8.1 \cdot 10^{-8}$ L mol⁻¹ s⁻¹. Once **Impurity 1** is formed, different active groups on the

Table 5 – Estimated parameters for suggested model

Reaction	Reaction expression	Kinetic constant/		Energy activation / kJ mol ⁻¹
(1) Catalyst complex formation	Ru + BINAP → Ru-BINAP	6.64E-09	L mol ⁻¹ s ⁻¹	114.63
(2) Catalyst activation	Ru-BINAP + H ₂ → Ru-BINAP*	0.2402	L mol ⁻¹ s ⁻¹	115.13
(3) Substrate degradation	Comp 1 → Imp 1	8.10E-08	s ⁻¹	77.96
(4) Impurity formation	Imp 1 + H ₂ → Imp 2	5.58E-06	L mol ⁻¹ s ⁻¹	132.58
(5) Substrate adsorption	Ru-BINAP* + Comp 1 ⇌ Ru-BINAP-Comp 1	1.18	L mol ⁻¹ s ⁻¹	131.60
(6) API product formation	Ru-BINAP-Comp 1 + H ₂ → Ru-BINAP-Comp 2	0.0518	L mol ⁻¹ s ⁻¹	107.00
(7) Substrate desorption	Ru-BINAP-Comp 2 ⇌ Ru-BINAP* + Comp 2	0.0139	L mol ⁻¹ s ⁻¹	100.25
(8) Transesterification	Comp 2 + TFE → Comp 3	2.01E-12	L mol ⁻¹ s ⁻¹	69.46

molecule are rapidly hydrogenated in reaction conditions into pseudo impurity – **Impurity 2** ($k_4 = 5.58 \cdot 10^{-6}$ L mol⁻¹ s⁻¹). The formation of **Compound 3** significantly increases with temperature ($E_{A,8} = 69.46$ kJ mol⁻¹), but in general is very slow ($k_8 = 2.01 \cdot 10^{-12}$ L mol⁻¹ s⁻¹). This compound is not considered an impurity, because in the next production step it can be converted into useful **Compound 5** by reaction ester hydrolysis.

Design space

In order to determine the desired operating conditions of the stereoselective hydrogenation of sitagliptine step during the scale-up process, mass balance and equipment needs to be considered to provide robust product quality with realistic and practical plant operating conditions. In order to simplify the representation of the design space, it was decided to specify maximum allowable levels for scale-up process. Temperature, T and hydrogen pressure, $p(\text{H}_2)$ and catalyst content (expressed as mol % to **Compound 1**), $w_{(\text{catalyst})}$ as main operating conditions were additionally explored through design space exploration (Fig. 6A, B, F). Followed by scale-up rules, it was necessary to maintain mixing properties (hydrodynamic). This was done by controlling gas mass transfer by controlling stirrer rotating speed in larger reactors in the region of mass transfer coefficient, $k_L a = 0.01$ s⁻¹. Mass transfer coefficient was also explored through space design (Fig. 6C).

Rather than shortening the reaction time, the reaction rate dependence on hydrogen pressure allows to lower the catalyst charge, which could be reduced while keeping the reaction time the same. If the pressure and temperature are varied, time to reach 99.9 % conversion is defined in the region of 15 to 20 hours (Fig. 6E). Longer time exhibits larger impurity quantities (**Impurity 2**) (Fig. 6D), so operating conditions must be set up regarding impu-

rity and yield as well. Temperature strongly affects reaction profile, especially on the optical purity (**Impurity 3**), but is limited with upper boundary, $T = 80$ °C which is boiling point of solvent. The chiral catalyst represents an important cost factor for the overall process so the quantity was maintained in the region of 1 mol % to **Compound 1**. Halving the catalyst level would increase the pressure to maintain the efficiency (Fig. 6F), but at the same time it would decrease the precious metals usage. This would affect the impurity production (Fig. 6D), and increase the waste that had to be treated, as well. Safety had to be considered also (mild operating conditions: low pressure and temperature), so the pressure region for hydrogen was set from 5.5 up to 6.5 bar, temperature 78 to 82 °C (Fig. 7 – green square), which gives the time of reaction of around 10–15 hours.

Impurity 2 was always present and its specification limit defined. During oxalate crystallization this impurity was removed from the product (mixture of **Compound 2** and **3**) with mother liquor, and does not affect final product impurity profile.

One set of laboratory experiments conducted to develop a model and fit the constants was used, and the further step was experimental verification, which was carried out at boundary conditions and at the centre of the proposed design space (Fig. 7). To represent process space on *Lab scale* in design space at conditions, $w_{(\text{catalyst})} = 1$ mol %, $k_L a = 0.01$ s⁻¹ and at the boundary edges of the rectangles, the experiments were conducted at temperature, $T = 80$ °C, and $p(\text{H}_2) = 6.0$ bar (Batch #1), and at temperature, $T = 75$ °C, and $p(\text{H}_2) = 6.5$ bar (Batch #2) (Fig. 7B). Scale-up process at *Pilot scale* was carried out at high catalyst content $w_{(\text{catalyst})} = 1$ mol %, $k_L a = 0.10$ s⁻¹ at $T = 80$ °C, and $p(\text{H}_2) = 6.0$ bar (Batch #3) and at temperature, $T = 80$ °C, and $p(\text{H}_2) = 6.5$ bar (Batch #4).

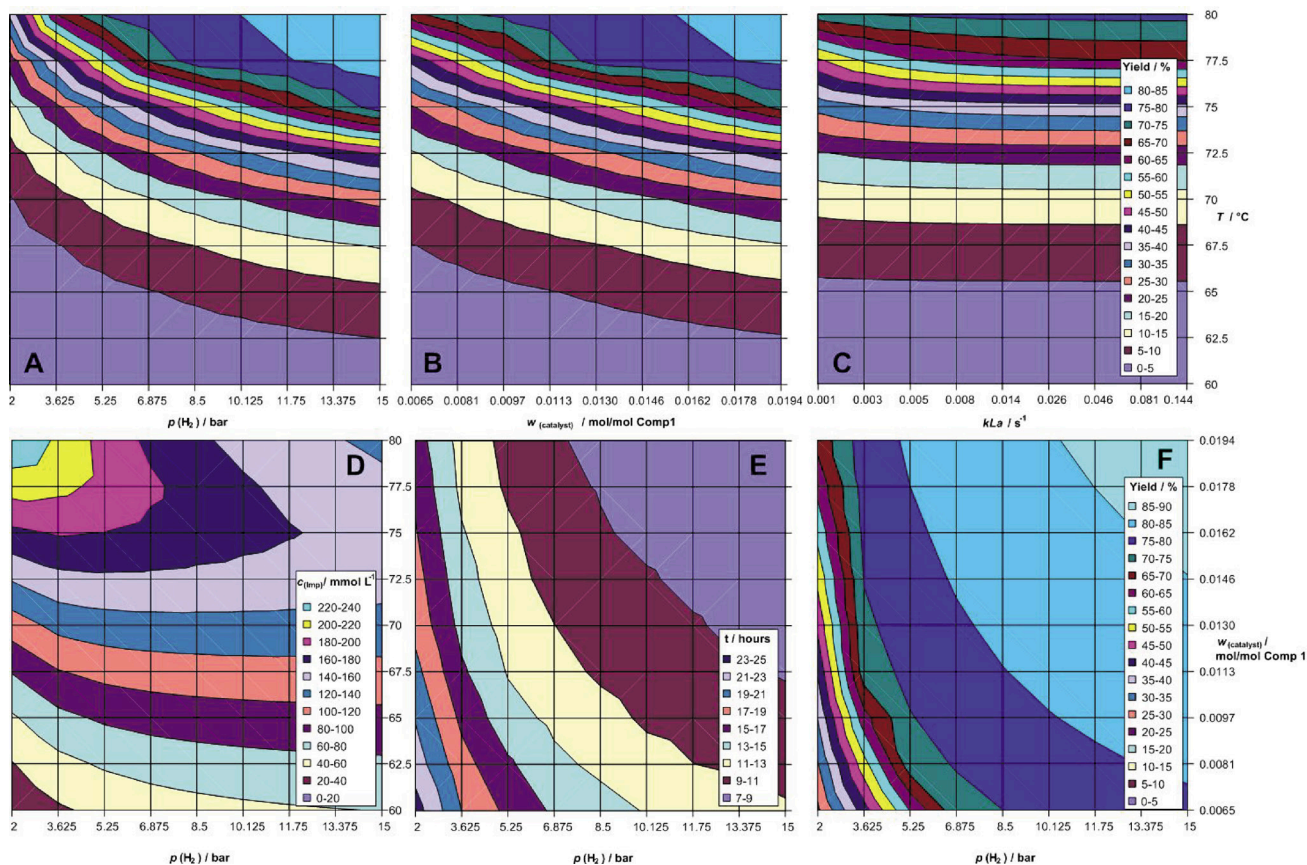


Fig. 6 – Response surface two-dimensional contour plots after 15 hours of stereoselective hydrogenation: A) Yield vs. pressure of hydrogen, $p(H_2)$ and temperature, T at percentage of catalyst, $w_{(catalyst)} = 1 \text{ mol } \%$, and mass transfer coefficient, $k_L a = 0.01 \text{ s}^{-1}$, B) Yield vs. $w_{(catalyst)}$ and T at $p(H_2) = 6 \text{ bar}$, and $k_L a = 0.01 \text{ s}^{-1}$, C) Yield vs. $k_L a$ and T at $p(H_2) = 6 \text{ bar}$, and $w_{(catalyst)} = 1 \text{ mol } \%$, D) Total impurity concentration, $c_{(imp2)}$ vs. $p(H_2)$ and T at $k_L a = 0.01 \text{ s}^{-1}$, $w_{(catalyst)} = 1 \text{ mol } \%$, E) Time, t to reach 99% conversion of Compound 1 vs. $w_{(catalyst)}$ and $p(H_2)$, at $T = 80 \text{ }^\circ\text{C}$, and $k_L a = 0.01 \text{ s}^{-1}$, and F) yield vs. $w_{(catalyst)}$ and $p(H_2)$, at $T = 80 \text{ }^\circ\text{C}$, and $k_L a = 0.01 \text{ s}^{-1}$

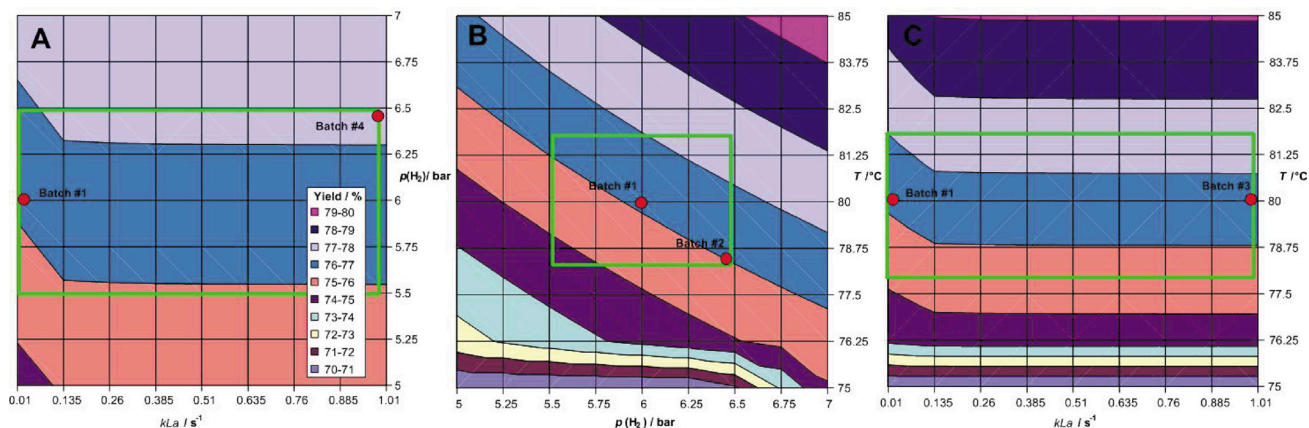


Fig. 7 – Definition of design space for the stereoselective hydrogenation based only on scale-up and quality considerations: A) Yield vs. $k_L a$, and $p(H_2)$ at $T = 80 \text{ }^\circ\text{C}$, B) Yield vs. $p(H_2)$ and T at $k_L a = 0.01 \text{ s}^{-1}$, and C) Yield vs. $k_L a$ and T at $p(H_2) = 6 \text{ bar}$, where green square is permitted range (reaction conditions: $w_{(catalyst)} = 1 \text{ mol } \%$)

While a design space affords an acceptable parameter space for laboratory batches, it also represents a set of the acceptable parameter space for scale-up (or down) batches. Scale-up to pilot batch with operating conditions: $T = 80 \text{ }^\circ\text{C}$, $w_{(catalyst)} = 1 \text{ mol } \%$, $p = 6 \text{ bar}$, showed different results (Fig. 7C, Table 5). On the macro-scale, where there is a large volume of reaction mixture, mass transfer

phenomena are crucial (mixing- hydrodynamics, turbulence, diffusion path, non-homogeneity, gas-liquid mass transfer etc.). Influence of mass transfer coefficient, $k_L a$, as a measure of mass transfer is significant. On the micro-scale which is connected with reaction kinetics, only intrinsic (kinetic) constants are significant, which are scale independent.

Conclusions

A case study of a QbD effort for the sitagliptine stereoselective hydrogenation step is provided. Understanding the functional relationship between process parameters as they progress through the manufacturing process through process modeling is the universal aspect of QbD for API development. The main task for engineers during the development is to include mathematical modeling, especially regarding computer predictive programs (*DynoChem*, *VisiMix*), to effectively eliminate as many of the CQAs and CPPs as possible from the API manufacturing process through continuous improvement efforts, or to bring the process in robust (safe) zone. Designed experiments generate the data required to establish a mathematic model, estimate the constants, and finally make the simulation from which the design space of manufacturing processes can be explored. This approach provides the process understanding that meets the production robustness and quality of final API product. Homogeneous asymmetric reduction of enamine can be divided into two steps: an initial induction period where activation of the catalyst occurs, and the reaction itself when the reduction of reactant occurs. When the whole process is considered, the catalyst complex formation is **r.d.s.**, where the value of the reaction rate constants is $k_1 = 6.64 \cdot 10^{-9} \text{ mol L}^{-1}\text{s}^{-1}$. If we consider only the reduction reaction of reactants, af-

ter the induction period, the desorption of the product from the catalyst is **r.d.s.**, with constant, $k_7 = 0.0139 \text{ L mol}^{-1} \text{ s}^{-1}$. Model predictions were combined with the anticipated acceptable quality attributes, practical plant operating conditions, and control capabilities to propose a process design space. In this case study, targeted points in process space were performed to obtain possible unknown parameter interactions. This mode of model use is verified according to the design space extremes, as well as at the target operating conditions.

Literature

1. Kremer, D. M., Hancock, B. C., *J. Pharm. Sci.* **95** (2006) 517.
2. Petrides, D. P., Koulouris, A., Lagonikos, P. T., *Pharm. Eng.* **22** (2002) 1.
3. ICH, International Conference On Harmonisation of Technical Requirements for the Registration of Pharmaceuticals for Human, Guide for ICH Q8/Q9/Q10 Implementation, http://www.ich.org/fileadmin/Public_Web_Site/ICH_Products/Guidelines/Quality/Q8_9_10_QAs/PtC/Quality_IWG_PtC-R2_6dec2011.pdf
4. Yu, L. X., *Pharm. Res.* **25** (2008) 781.
5. Lepore, J., Spavins, J., *J. Pharm. Innov.* **3** (2008) 79.
6. Ganzer, W. P., Materna, J. A., Mitchell, M. B., Wall, L. K., *Pharm. Technol.* **2** (2005) 46.
7. Seibert, K. D., Sethuraman, S., Mitchell, J. D., Griffiths, K. L., McGarvey B., *J. Pharm. Innov.* **3** (2008) 105.
8. Garcia, T., Cook, G., Nosal, R., *J. Pharm. Innov.* **3** (2008) 60.
9. Trivedi, B., *Int. J. Pharm. Pharm. Sci.* **4** (2012) 17.
10. U. S. Department of Health and Human Services Food and Drug Administration, Guidance for Industry, Process Validation: General Principles and Practices, (2011) <http://www.fda.gov/downloads/Drugs/GuidanceComplianceRegulatoryInformation/Guidances/ucm070336.pdf>
11. Ende, D., Bronk, K. S., Mustakis, J., O'Connor, G., Santa Maria, C. L., Nosal, R., Watson, T. J.N., *J. Pharm. Innov.* **2** (2007) 71.
12. Brueggemeier, S. B., Reiff, E. A., Lyngberg, O. K., Hobson, L. A., Tabora, J. E., *Org. Process Res. Dev.* **16** (2012) 567.
13. Castagnoli, C., Yahyah, M., Cimarosti, Z., Peterson, J. J., *Org. Process Res. Dev.* **14** (2010) 1407.
14. Burt, J. L., Braem, A. D., Ramirez, A., Mudryk, B., Rossano, L., Tummala, S., *J. Pharm. Innov.* **6** (2011) 181.

Table 6 – Confidence intervals for suggested model

Number of parameters	16
Number of data points	448
Degrees of freedom	432
SSQ	27.911
F-statistic	411.087
F-critical	1.667
D, serial correlation of residuals	0.2467
Norm. kurtosis of residuals	81.487
Norm. skewness of residuals	0.078

Table 7 – Processing conditions chosen for the lab and pilot batches and the resulting reaction yield, chromatographic and optical purity results

Scale	Time of reaction/ hours	Batch	Yield _(calc.) %	Yield _(exp.) %	HPLC/ chrom. purity %		HPLC/ opt. purity %
					Comp. 2	Comp. 3	
Lab (<i>FlexyLab</i>)	20	#1	76.1	76.3	88.6	9.9	99.6
	20	#2	77.1	77.1	88.8	10.0	99.6
Pilot (<i>PfauDler</i>)	15	#3	77.8	78.2	90.9	6.7	99.6
	15	#4	78.2	78.5	93.4	5.7	99.6

15. Cimarosti, Z., Bravo, F., Stonestreet, P., Tinazzi, F., Vecchi, O., Camurri, G., *Org. Process Res. Dev.* **4** (2010) 993.
16. Looby, M., Ibarra, N., Pierce, J. J., Buckley, K., O'Donovan, E., Heenan, M., Moran, E., Farid, S. S., Baganz, F., *Biotechnol. Progr.* **27** (2011) 1718.
17. Wu, H., White, M., Khan, M. A., *Int. J. Pharm.* **405** (2011) 63.
18. Schmidt, B., Patel, J., Ricard, F. X., Brechtelsbauer, C. M., Lewis, N., *Org. Process Res. Dev.* **8** (2004) 998.
19. S. P. Miksinski: Regulatory Assessment of Applications Containing QbD Elements – Reviewer Experience, FDA/CDER, (2012), Chicago.
20. Herman, G. A., Stevens, C., Van Dyck, K., Bergman, A., Yi, B., De Smet, M., Snyder, K., Hilliard, D., Tanen, M., Tanaka, W., Wang, A. Q., Zeng, W., Musson, D., Winchell, G., Davies, M. J., Ramael, S., Gottesdiener, K. M., Wagner, J. A., *Clin. Pharmacol. Ther.* **78** (2005) 675.
21. Dunn, P. J., Wells, A. S., Williams, M. T. “Green Chemistry in the Pharmaceutical Industry”, Wiley-VCH, Weinheim, 2010.
22. Hansen, K. B., Hsiao, Y., Xu, F., Rivera, N., Clausen, A., Kubryk, M., Krska, S., Rosner, T., Simmons, B., Balsells, J., Ikemoto, N., Sun, Y., Spindler, F., Malan, C., Grabowski, E. J. J., Armstrong, J. D. III, *J. Am. Chem. Soc.* **131** (2009) 8798.
23. Lee, N. E., Buchwald, S. L., *J. Am. Chem. Soc.* **116** (1994) 5985.
24. Tararov, V. I., Kadyrov, R., Riermeier, T. H., Holz, J., Bornner, A., *Tetrahedron Lett.* **41** (2000) 2351.
25. Lubell, W. D., Kitamura, M., Noyori, R., *Tetrahedron: Asymmetry* **2** (1991) 543.
26. Schultz, C. S., Krska, S. W., *Acc. Chem. Res.* **40** (2007) 1320.
27. Hsiao, Y., Rivera, N. R., Rosner, T., Krska, S. W., Njolito, E., Wang, F., Sun, Y., Armstrong, J. D. III, Grabowski, E. J. J., Tillyer, R. D., Spindler, F., Malan, C., *J. Am. Chem. Soc.* **126** (2004) 9918.
28. Clausen, A. M., Dziadul, B., Cappuccio, K. L., Kaba, M., Starbuck, C., Hsiao, Y., Dowling, T. M., *Org. Process Res. Dev.* **10** (2006) 723.
29. Ertl, G., Knözinger, H., Weitkamp, J., *Handbook of Heterogeneous Catalysis*; Wiley-VCH, Weinheim, 1997.
30. Baehr, H. D., Stephan, K., “Heat and Mass Transfer”, 2nd Ed., Springer, Berlin Heidelberg, 2006.
31. Griskey, R. G., “Transport phenomena and unit operations”, John Wiley & Sons, Inc., New York, 2002.
32. Šunjić, V., Parnham, M. J., “Signposts to Chiral Drugs” Springer, Basel, 2011.
33. King, S. A., Armstrong, J., Keller, J., *Org. Synth.* **81** (2005) 78.